

## Electronic Supplementary Information (ESI)

### **Rapid Exfoliation for Few-layer Enriched Black Phosphorus Dispersion via Superhydrophobic Silicon-nanowire-embedded Microfluidic Process**

Chang-Ho Choi <sup>\*, a, ,</sup> Dong-Hyeon Ko,<sup>b</sup> Ho Young Jun,<sup>c</sup> Si Ok Ryu,<sup>c</sup> Dong-Pyo Kim<sup>\*,b</sup>

a Department of Chemical Engineering, Gyeongsang National University, Jinju-daero, 501, Jinju-Si, Gyeongsangnam-do, South Korea

b National Center for Intelligent Microprocess of Pharmaceutical Synthesis, Department of Chemical Engineering, Pohang University of Science and Technology (POSTECH), Pohang, 37673, Korea

c Department of Chemical Engineering, Youngnam University, 280, Daehak-ro, Gyeongsangsi, Gyeongsangbuk-do, South Korea

E-mail: [ch\\_choi@gnu.ac.kr](mailto:ch_choi@gnu.ac.kr), [dpkim@postech.ac.kr](mailto:dpkim@postech.ac.kr)

## Section 1. 7-Hydroxycoumarin (7-HC) fluorescence emission spectra

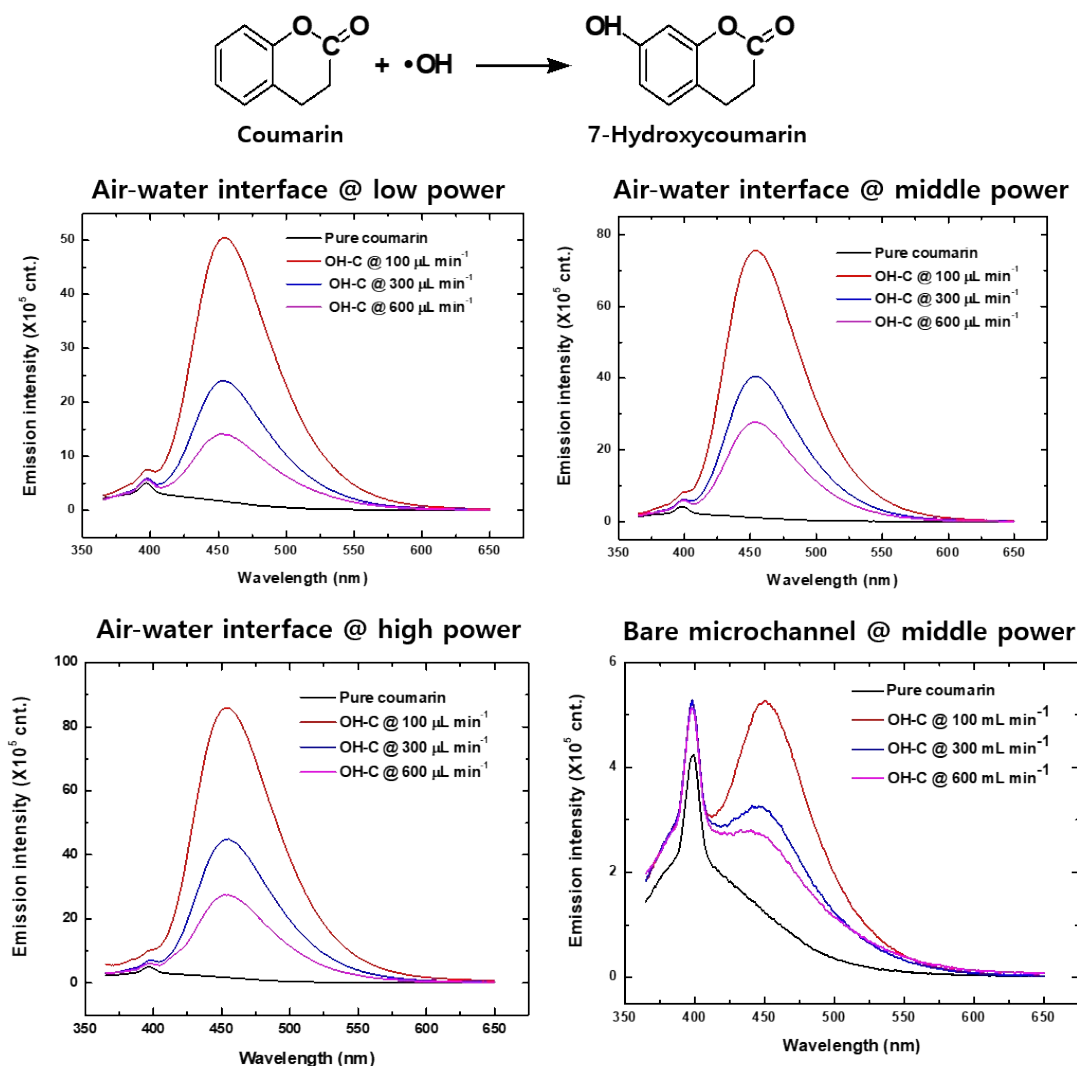


**Figure S1.** 7-HC fluorescence emission spectra obtained from air-water fluidic interface and bare microchannel device at a different sonic power density values (experimental conditions: ultrasonic wave frequency: 40 kHz and temperature: 25 °C).

The emission rate of 7-HC in Figure 1 is derived by dividing the PL intensity value at a wavelength of 452 nm by the residence times of 5 s, 10 s, and 30 s that correspond to the flow rates of 600  $\mu\text{L min}^{-1}$ , 300  $\mu\text{L min}^{-1}$ , and 100  $\mu\text{L min}^{-1}$ , respectively.

## Section 2. Dimensional analysis of a typical Bulk BP

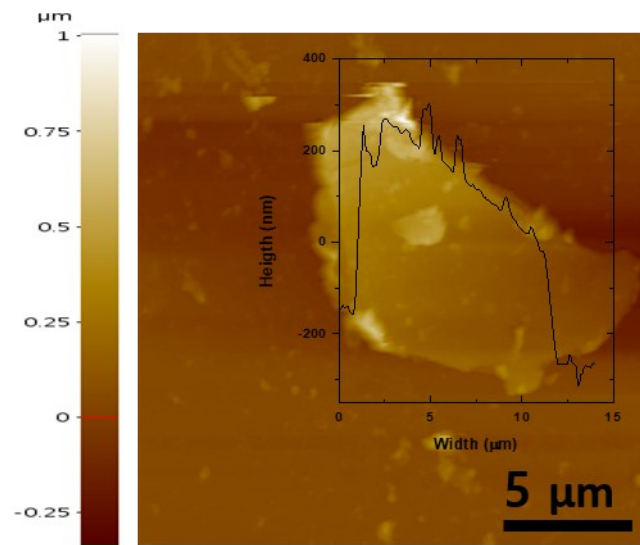


**Figure S2.** AFM analysis of a typical bulk BP prior to fragmentation.

### Section 3. Fragmentation efficiency calculation of BP in the superhydrophobic SiNW microfluidic system

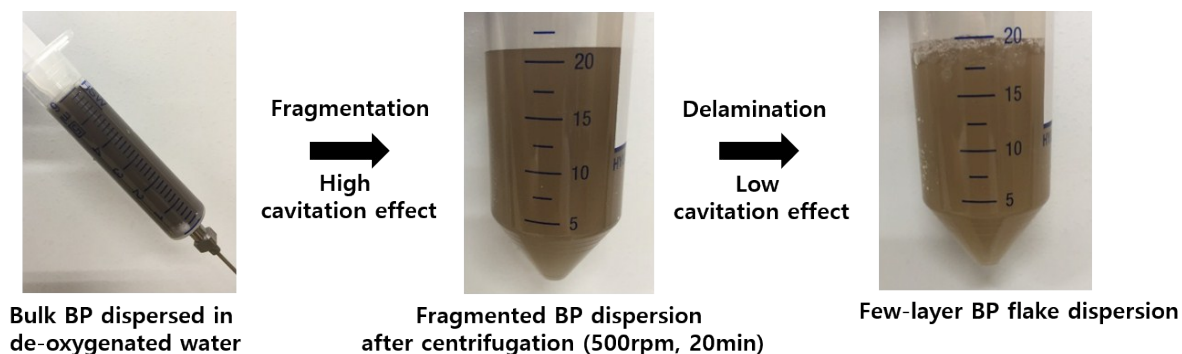


**Figure S3.** Optical images of bulk BP dispersed in de-oxygenated water, fragmented BP dispersion after centrifugation at 500 rpm for 20 min, and few-layer BP flake dispersion.

**Table S1.** Quantitative fragmentation efficiency of the bulk BP *via* the superhydrophobic SiNW microfluidic system at high power density for 30 s.

Fragmentation cycle	Initial amount (mg)	Initial concentration (mg/mL)	Filtered BP (mg)	Fragmented BP (mg)	*Fragmentation efficiency (%)
1			1.71	1.29	43.1
2			1.27	1.73	57.6
3	3	0.5	0.95	2.05	68.1
4			0.76	2.24	74.6
5			0.61	2.39	79.5

\* Fragmentation efficiency presents the average value of the fragmentation efficiency obtained after performing three experiments at each cycle.

## Section 4. Dimensional analysis of the fragmented BP

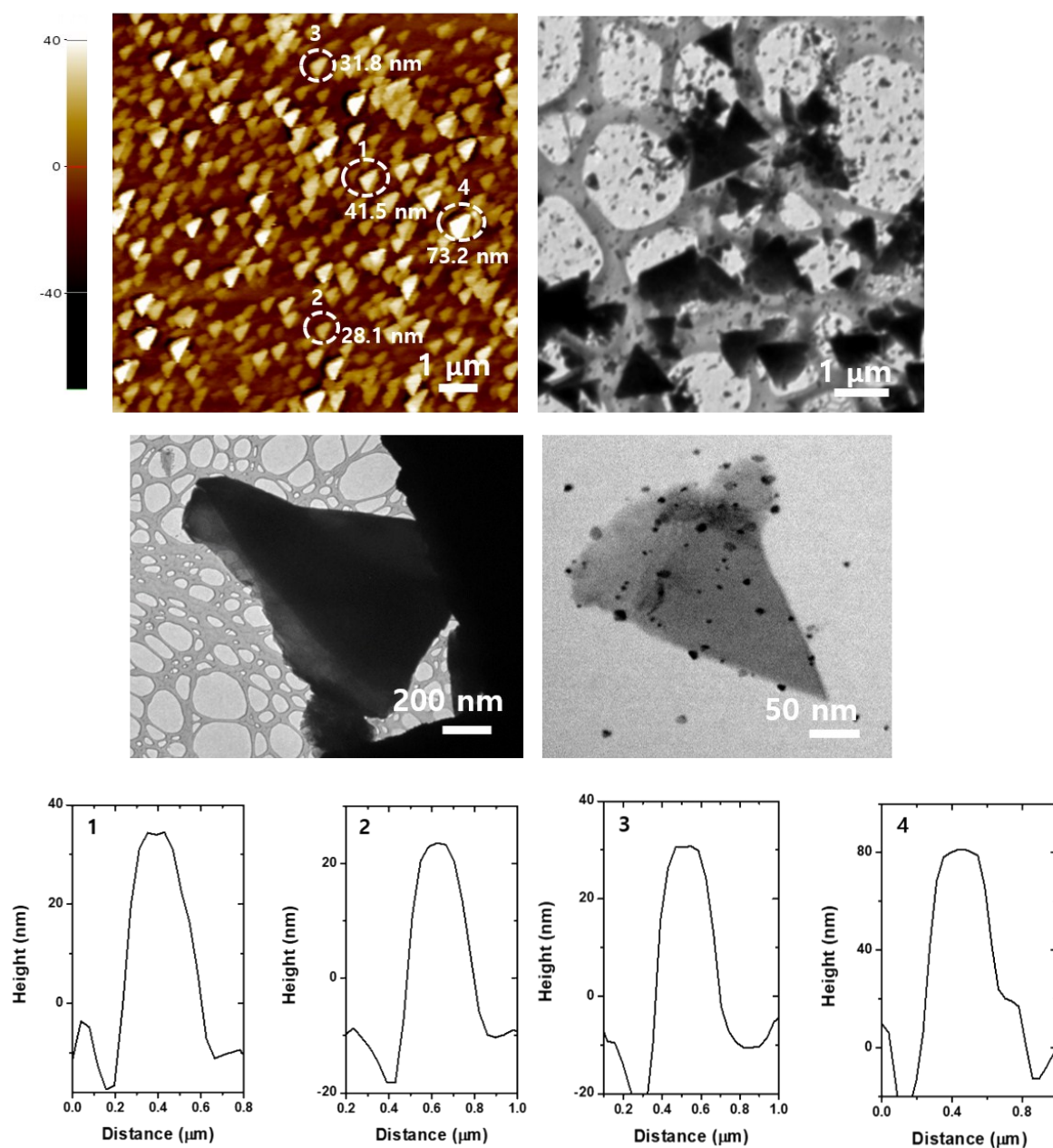


**Figure S4.** TEM and AFM images of the fragmented BPs with triangular structure.

## Section 5. Dimensional analysis of the few-layer BP flakes

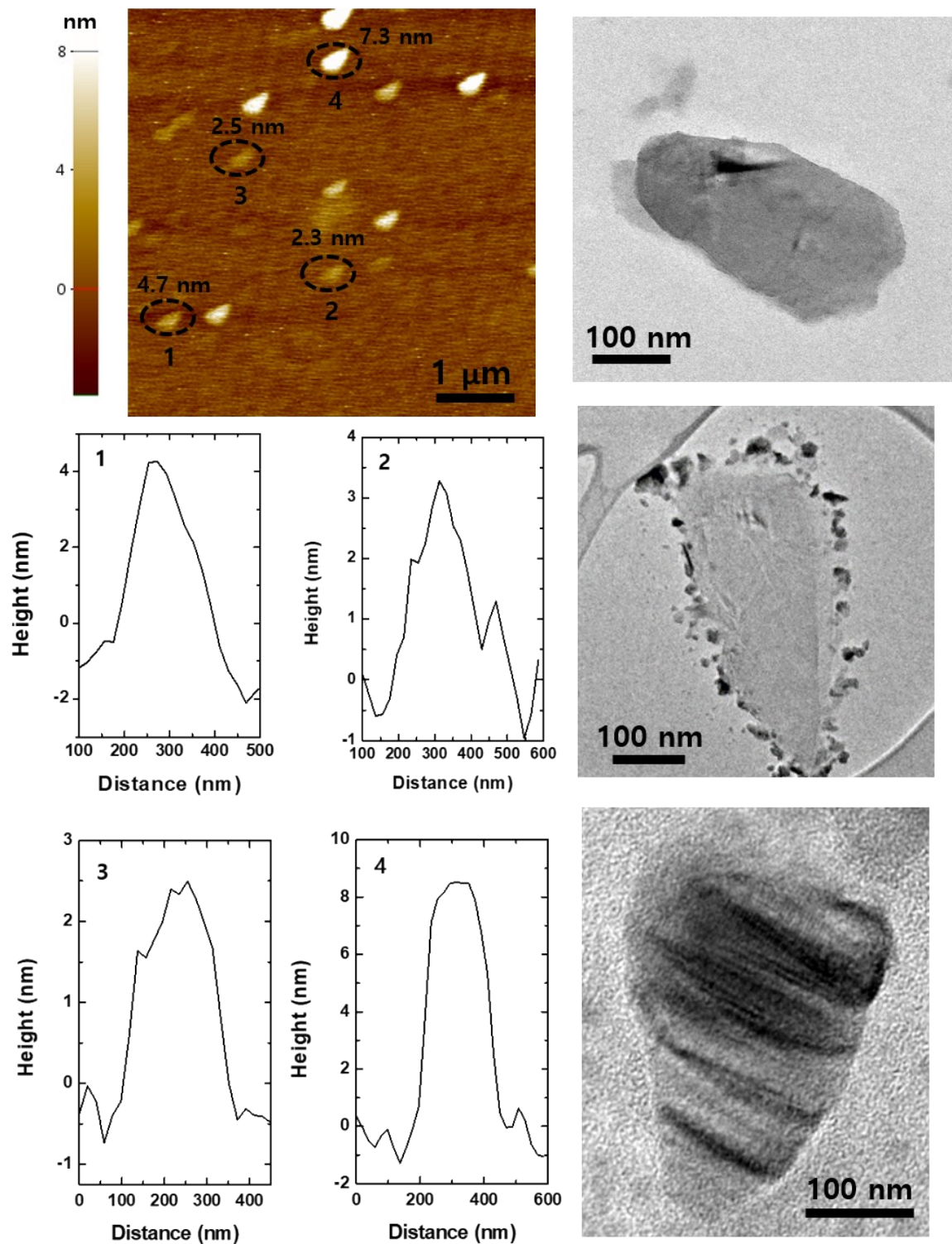
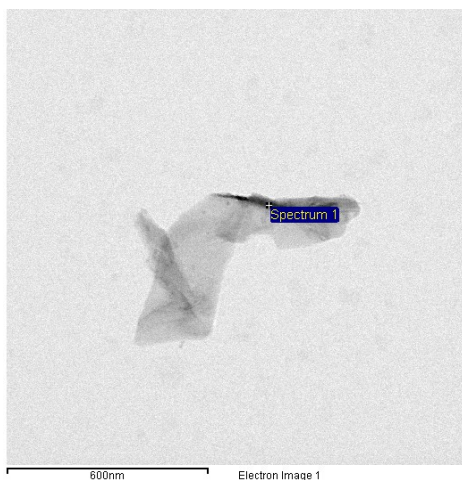


**Figure S5.** AFM image and dimensional analysis of the few-layer BP flakes.

## Section 6. EDS analysis of the few-layer BP flake



Element	Weight%	Atomic%
O K	6.37	11.63
P K	93.63	88.37
Totals	100.00	

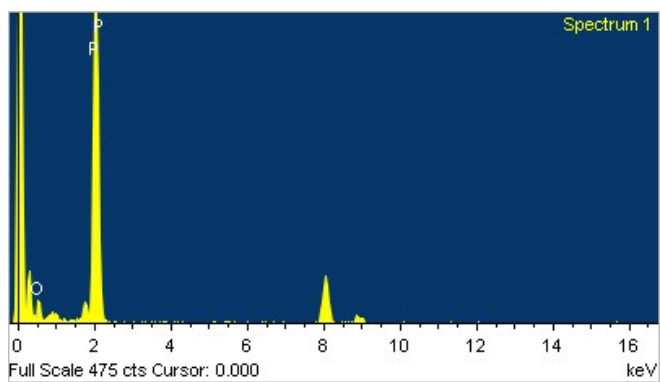


**Figure S6.** EDS analysis of a typical few-layer BP flake.

## Section 7. Characteristic results of BP nanodots delaminated at the high cavitation effect

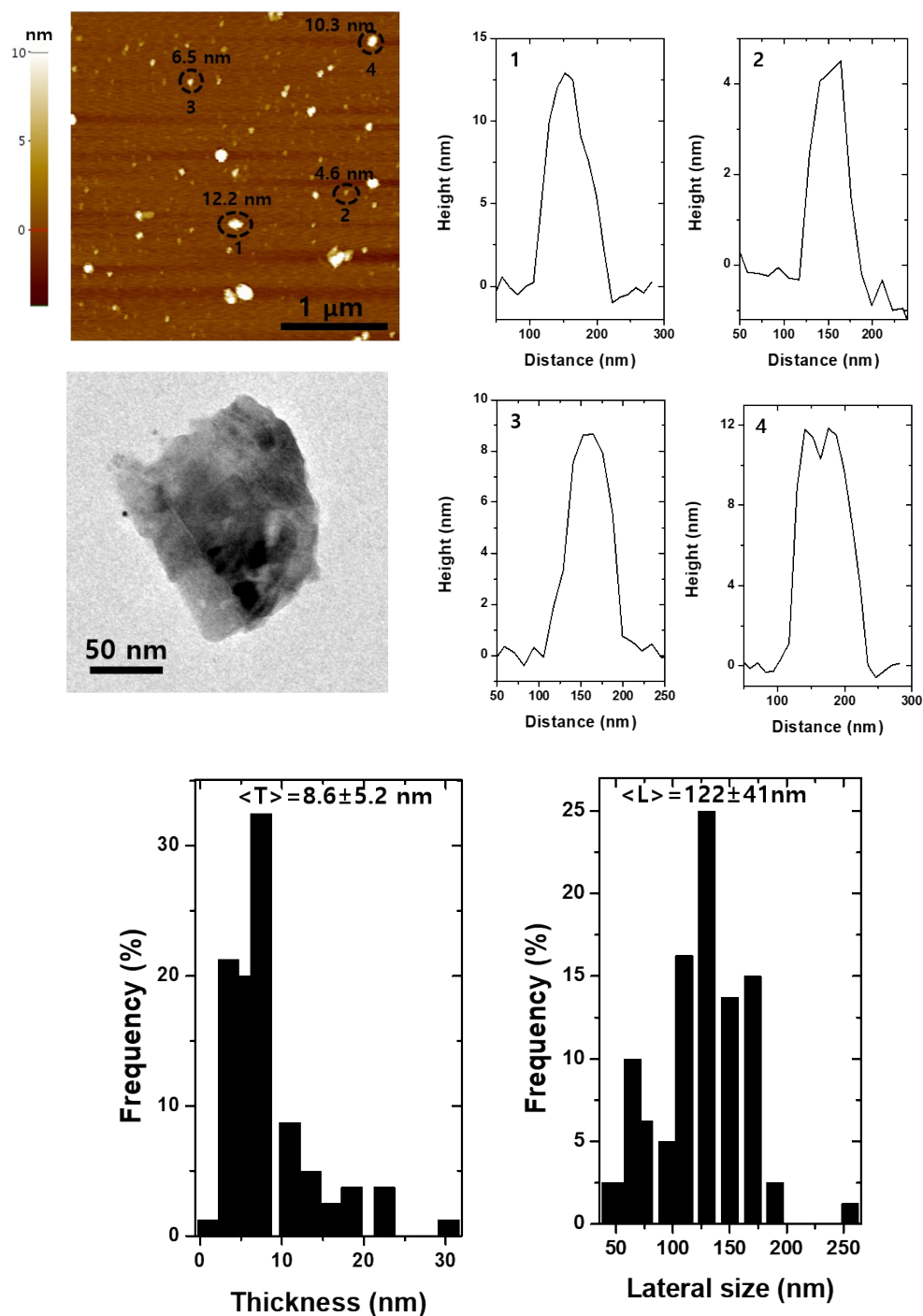


**Figure S7.** Characteristics of BP nanodots delaminated at high cavitation effect: AFM image, TEM image, and statistical dimensional analysis (statistical dimensional analysis was performed by counting 200 individual BP nanodots).

Section 8. Characteristic results of BP delaminated at the middle cavitation effect

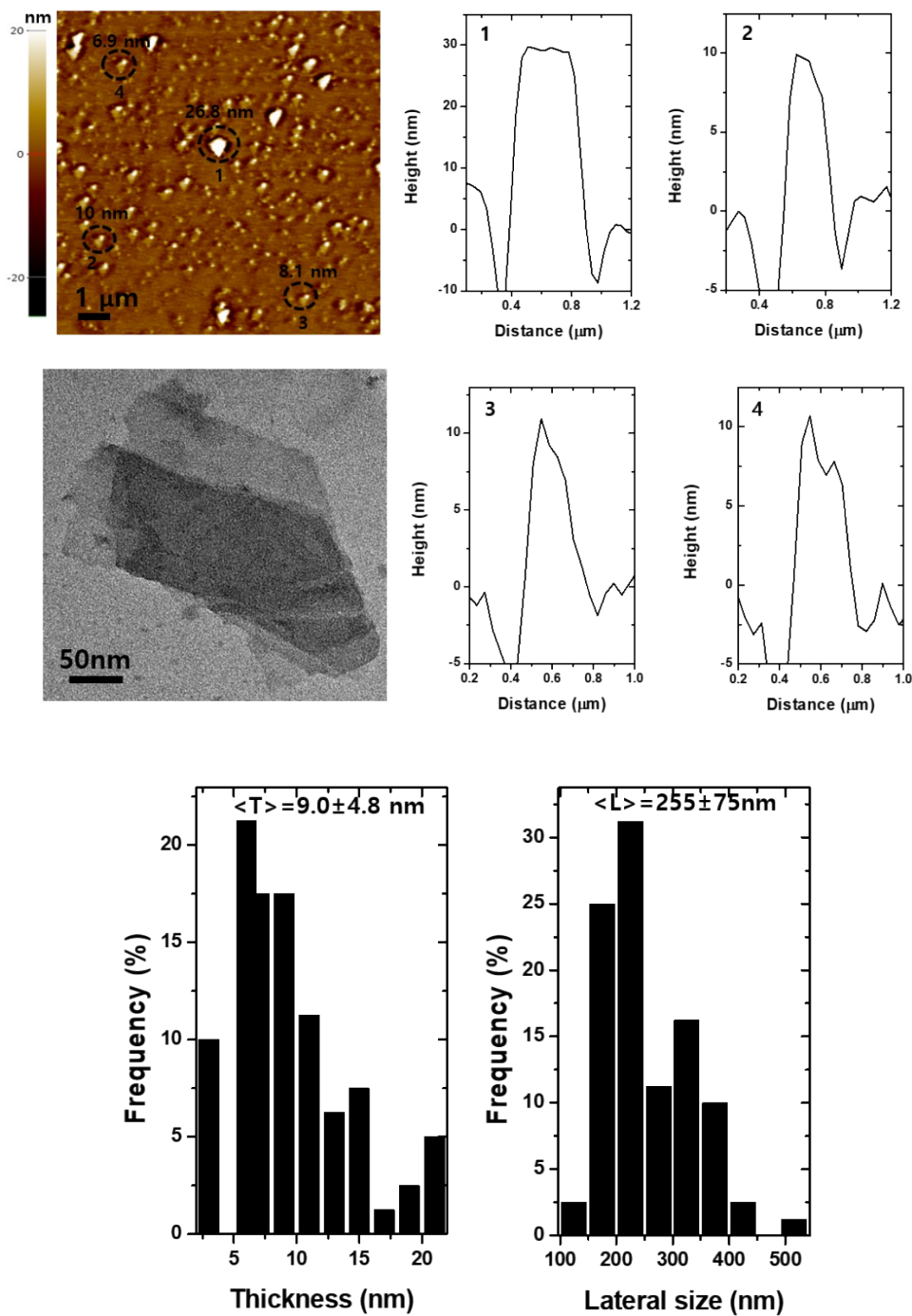


**Figure S8.** Characteristics of BP delaminated at middle cavitation effect: AFM image, TEM image, and statistical dimensional analysis (statistical dimensional analysis was performed by counting 200 individual BP).

## Section 9. Characteristic results of BP delaminated at low cavitation effect

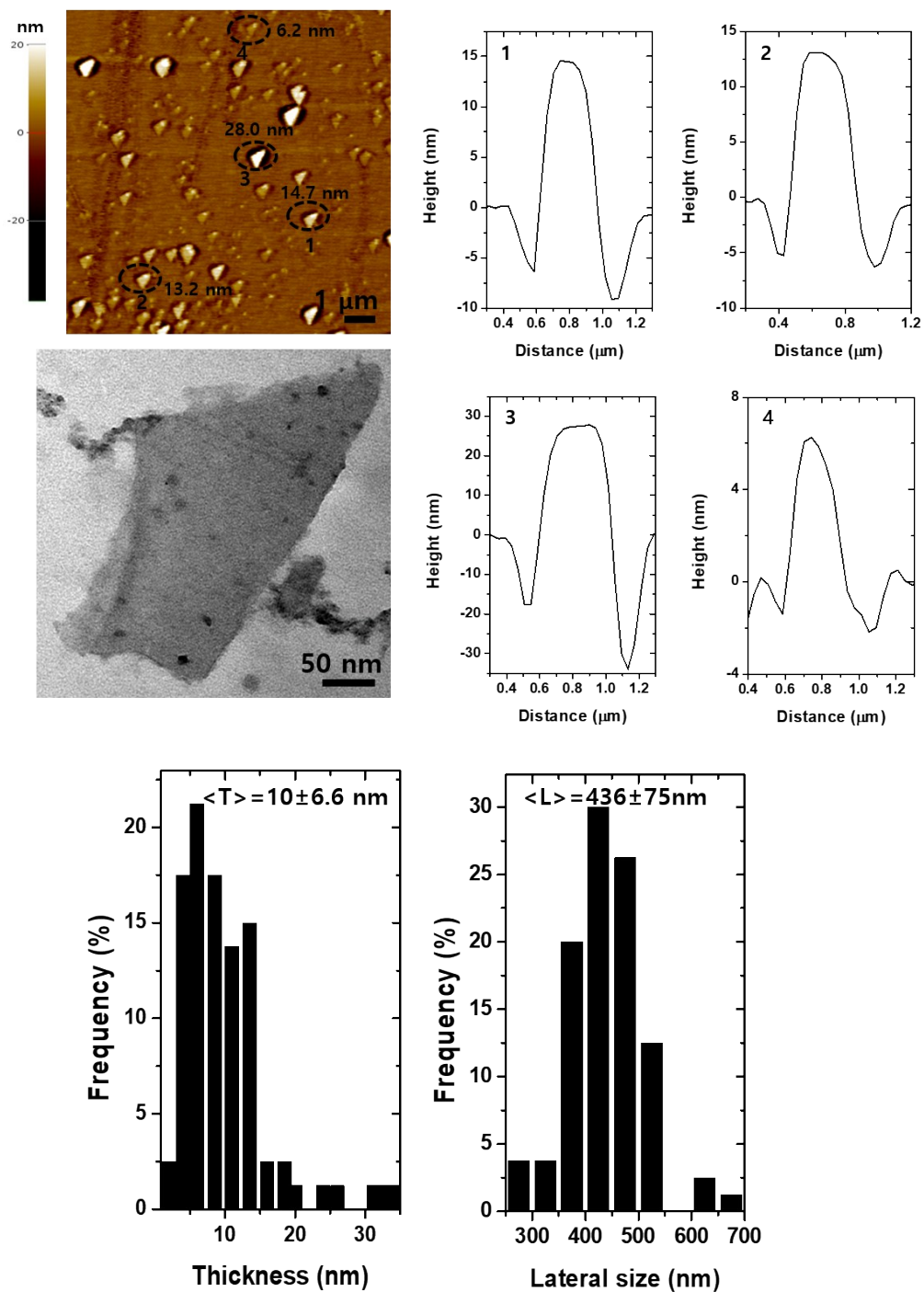


**Figure S9.** Characteristics of BP delaminated at low cavitation effect: AFM image, TEM image, and statistical dimensional analysis (statistical dimensional analysis was performed by counting 200 individual BP).

## Section 10. Stability of the few-layer BP flake dispersions

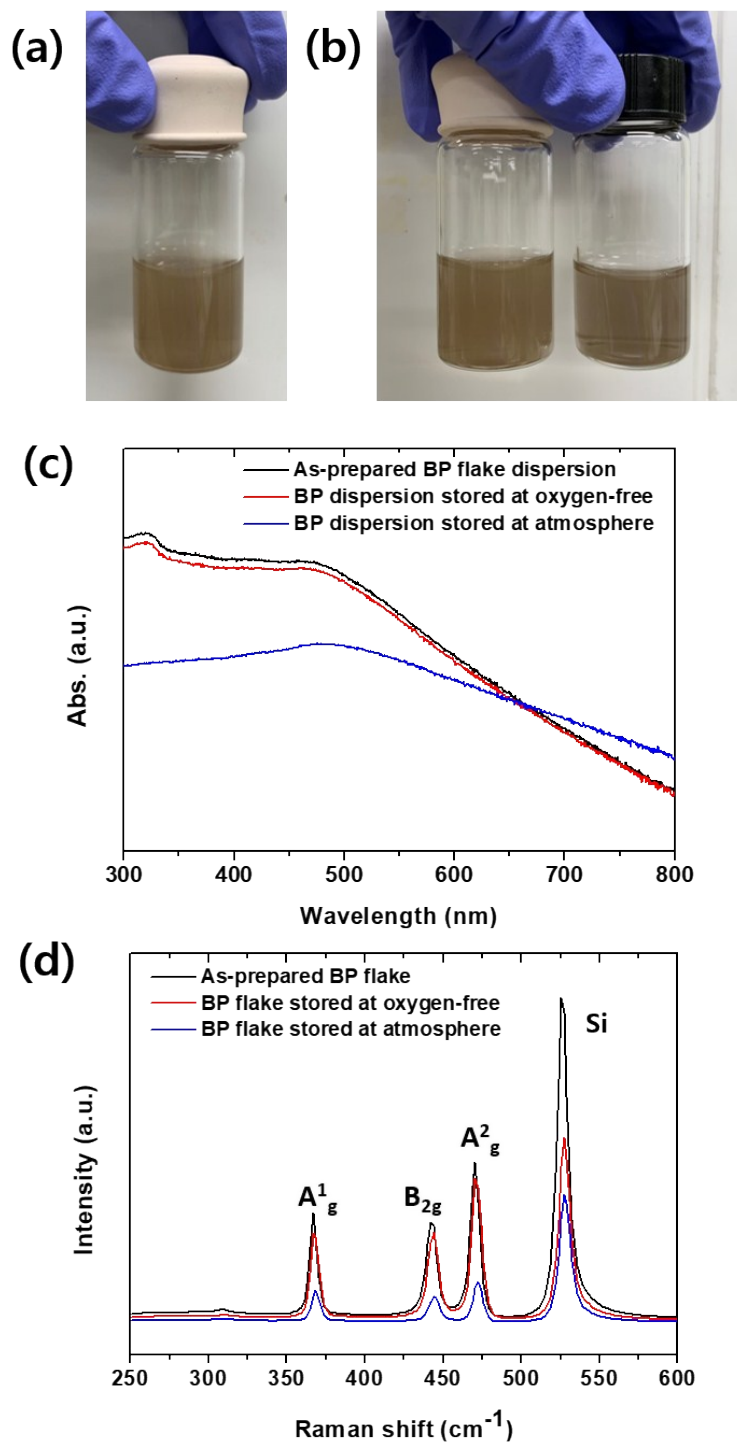


**Figure S10.** Stability evaluation of the few-layer BP flakes: Optical image of (a) as-prepared BP flake dispersion and (b) BP flake dispersion stored at oxygen-free (left) and BP flake dispersion stored at atmosphere (right). (c) UV-Vis absorption spectra of the BP flake and (d) Raman spectra of the few-layer BP flake dispersion stored at different condition.

## Section 11. Durability of the superhydrophobic SiNWs

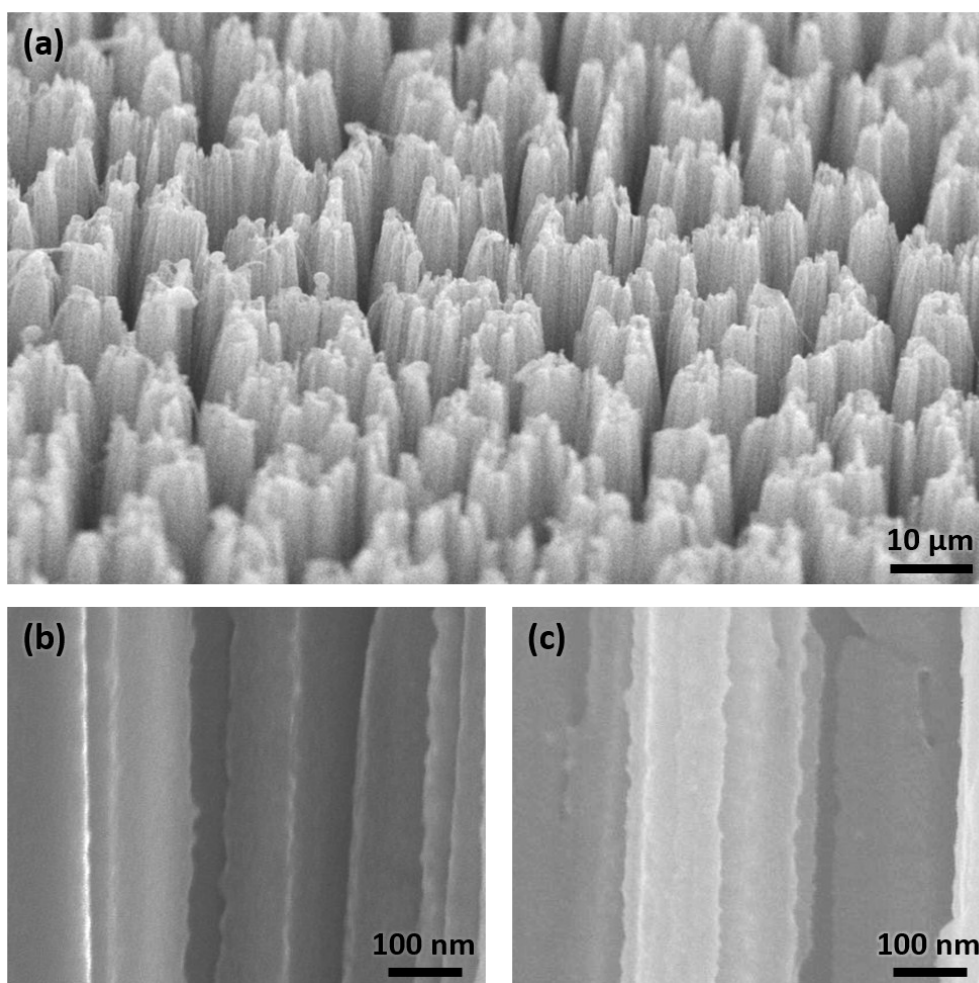


**Figure S11.** (a) Tilted view of SEM image of SiNW surface after the exfoliation processes was repeated ten times, Magnified view of SiO<sub>2</sub>-nanoparticle-decorated SiNWs (b) before and (c) after exfoliation process was repeated ten times.

## Section 12. Schematic of a superhydrophobic SiNW microfluidic system

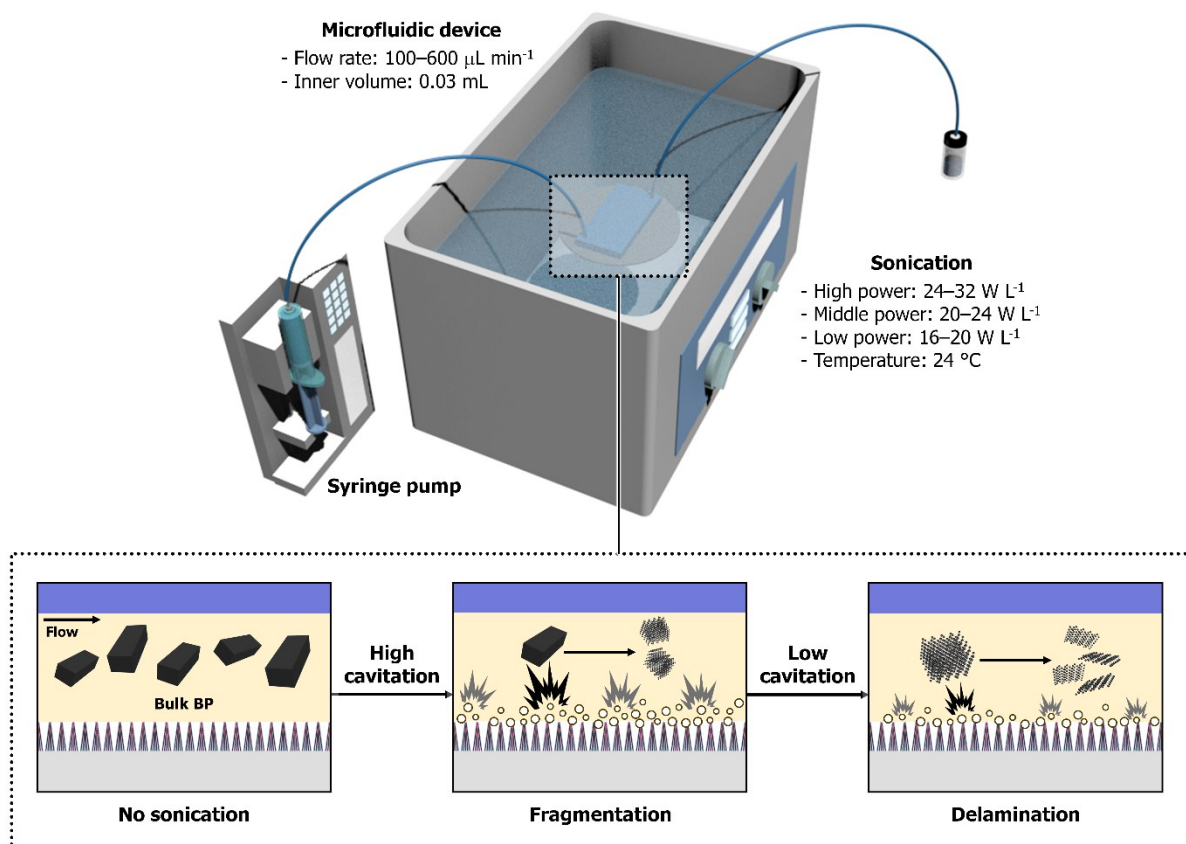


**Figure S12.** Schematic of the superhydrophobic SiNW microfluidic system to fragment bulk BP and delaminate the fragmented BP into few-layer BP flakes.